Relationship between Molecular and Cellular Dissociation Rates for VLA-4/VCAM-1 Interaction in the Absence of Shear Stress

Gordon Zwartz,* Alexandre Chigaev,* Terry Foutz,* Richard S. Larson,* Richard Posner,† and Larry A. Sklar*
*Department of Pathology and Cancer Center, University of New Mexico Health Sciences Center, Albuquerque, New Mexico; and †Department of Chemistry, Northern Arizona University, Flagstaff, Arizona

ABSTRACT The rate of leukocyte recruitment to and detachment from the vasculature contributes to cellular tethering, rolling, firm adherence, and migration across an endothelium layer. The molecular rates depend on the type and number of bound integrin or selectin adhesion molecules, shear force acting on the bound adhesion molecules, and affinity state of integrins. Although little is known of the effect that the number of adhesion molecules has on leukocyte recruitment, it has been shown that firm adhesion for cells in suspension may be mediated by small numbers of bound adhesion molecules. We studied the disaggregation of aggregates composed of B78H1 cells transfected with human vascular cell adhesion molecule-1 (VCAM-1) and human monoblastoid U937 cells expressing Very Late Antigen-4 (VLA-4). Aggregate disaggregation rates were obtained and compared to dissociation rates for soluble rhVCAM-1 ligand and monoblastoid U937 cells. Under conditions without shear stress, it was found that average cellular disaggregation rates were a factor of 1.3 ± 0.4 times slower than molecular dissociation rates for the 1 mM Mn^{2+} and 1 mM Mn^{2+} + 1 mM Ca^{2+} conditions. A simple mathematical model was used to predict how much smaller the dissociation constant would be if the number of bonds holding an aggregate varied from one bond to *N* bonds under conditions without shear stress. The average number of adhesion bonds holding the cell aggregates together was found to be 1.5 ± 0.7. This suggests that a few bonds were needed to form cellular aggregates and that increased aggregation was related to integrin affinity changes and not due to clustering or increased bond numbers.

INTRODUCTION

Cell adhesion molecules form a receptor-counterstructure complex that allows cells to bind to other cells and to extracellular matrix. Leukocyte adhesion to vascular endothelium involves four families of adhesion molecules—selectins and their glycoprotein ligand counterstructures, and integrins and their Ig superfamily counterstructures. Selectins tend to regulate leukocyte tethering and rolling whereas integrins typically regulate firm attachment. The sequence of events involved in leukocyte adhesion including signaling from chemokine receptors has been referred to as ''traffic signals.'' Understanding how adhesion molecules attach and de-attach under variations of integrin affinity, receptor site density, and shear stress will lead to a better understanding of the mechanisms by which cells migrate, differentiate, and participate in cancer metastasis, hemostasis, wound healing, inflammation, host defense, and development (Brakebusch et al., 2002; McEver, 2001).

Integrins are of special interest because their activity is highly regulated. Integrins are $\alpha\beta$ heterodimers comprised of at least eight different β and 18 α chains and forming at least 22 $\alpha\beta$ pairs (Chothia and Jones, 1997; Haas and Plow, 1994; Shyy and Chien, 2002). The α4 integrin, particularly $\alpha4\beta1$ (Very Late Antigen-4; VLA-4) is reported to exist in multiple affinity states. Lower affinity state(s) are associated with rolling and higher affinity state(s) with firm adhesion (Chen et al., 1999). The binding of VLA-4 to its counterstructure vascular cell adhesion molecule-1 (VCAM-1) is important in inflammatory and allergic responses. The affinity of VLA-4 for an LDV-containing small molecule and native VCAM-1 ligand on living cells has been determined (Chigaev et al., 2001). These results show that the affinity of VLA-4 is regulated in the presence of divalent cations such as Ca^{2+}, Mn^{2+}, Mg^{2+}, and by chemokines. Moreover, VLA-4 avidity has been correlated with affinity in cells in suspension based on disaggregation rates between U937 cells (expressing VLA-4) and B78H1 cells (transfected withVCAM-1; Chigaev et al., 2003a).

A receptor-ligand bond is characterized by a dissociation constant K_d. The dissociation rate constant can be estimated by measuring the bond formation in forward (k_{on}) and dissociation in reverse (k_{off}) reactions. A direct measurement of cell avidity can be obtained from the rate of the disaggregation of cell aggregates (k_{disagg}). Depending on receptor surface density and shear, cell aggregates may form multiple adhesion bonds, so that a measurement of k_{disagg} for cell aggregates reflects the number of bonds holding the aggregate together under conditions where molecular rebinding is prohibited. The more bonds formed between cells the smaller the measured k_{disagg}. By using mathematical models (Piper et al., 1998) it is possible to deduce the number of bonds holding cell aggregates together and thus obtain intrinsic properties of adhesion molecules.

Several experimental techniques have been used to measure k_{off} values for a variety of selectin and integrin adhesion molecules (Alon et al., 1997; Chang et al., 2000; Chateau et al., 2001). The calculation of the force acting on the

Submitted April 2, 2003, and accepted for publication October 14, 2003.

Address reprint requests to Prof. Larry A. Sklar, Department of Pathology and Cancer Center, University of New Mexico HSC, Albuquerque, NM 87131. Tel.: 505-272-4249; Fax: 505-272-6995; E-mail address: lsklar@salud.unm.edu.

0006-3495/04/02/1243/10 $2.00

adhesion bonds can be estimated for each experimental technique, thus making comparisons between experimental techniques straightforward. It was observed that smaller k_{disagg} values are associated with firmly adhering cells whereas larger k_{disagg} values are associated with rolling or tethering cells (Chateau et al., 2001). The difficulty in using these data to obtain molecular properties of the adhesion molecules stems from the inability to isolate single adhesion bonds and study them under defined conditions (Zhu et al., 2002). We did not attempt to simulate single bond conditions but we did maintain cells in suspension, without shear force conditions, and under normal receptor and ligand densities. Then we compared k_{off} values from experiments measuring VCAM-1 and cells (single bond formation; Chigaev et al., 2003a) to k_{disagg} of cellular aggregates (multibond formation). These molecular dissociation measurements of VLA-4 were made with human vascular adhesion molecule-FITC (VCAM-FITC) and by competitive experiments using FITC conjugated derivative of the LDV-containing small molecule and soluble recombinant VCAM-1 (rhVCAM-1). A mathematical model used the difference in k_{off} values between single bonds (data obtained from soluble ligand experiments) and multiple bonds (data obtained from cellular experiments) to estimate the number of bonds. Consequently, we were able to derive molecular properties of bonds without manipulating experimental conditions to achieve single bond formation. The affinity of VLA-4 is regulated in the presence of Ca^{2+} and Mn^{2+} divalent cations. As cellular disaggregation rates for aggregate and dissociation rates for soluble rhVCAM-1 data were found to be different, we were able to predict that a small number of bonds were responsible for holding cell aggregates together.

MATERIALS AND METHODS

Cell lines and transfectant construct

Human monoblastoid line U937 expressing human VLA-4 integrin and mouse melanoma cell line B78H1 (purchased from ATCC, Rockville, MD) and were transfected with human VCAM-1 (Chigaev et al., 2001). For transfection of B78H1 cells, full-length human VCAM-1 cDNA was a kind gift from Dr. Roy Lobb of Biogen. The original construct (Osborn et al., 1989) was subcloned into the pTRACER vector, Invitrogen (Carlsbad, CA). Transfection into B78H1 was done using the Lipofectamine Reagent Gibco (Grand Island, NY). High expressors were selected using the MoFlo Flow Cytometer, Cytomation (Fort Collins, CO). Cells grown in RPMI 1640 (supplemented with 0.7 mg/ml Zeocin (Invitrogen, Carlsbad, CA), 2 mM L-glutamine, 100 units/mL penicillin, 100 μg/mL streptomycin, 10 mM HEPES, pH 7.4, and 10% heat inactivated fetal bovine serum) were harvested and resuspended in 1 ml of HEPES buffer (110 mM NaCl, 10 mM KCI, 10 mM glucose, 1 mM $MgCI_2$, and 30 mM HEPES, pH 7.4) containing 10 mM glucose and 0.1% HSA and stored on ice.

Antibodies and peptides

Binding between VLA-4 and VCAM-1 was blocked using a VLA-4 specific peptide [4-(n'-2-methyphenyl)ureido)-phenylacetyl-L-leucyl-L-asparty-L-valyl-L-prolyl-L-alanyl-L-alanyls-L-lysine]. This LDV-containing small molecule was synthesized at Commonwealth Biotechnologies (Richmond, VA). Antibodies blocking β2 were anti-human β2 integrin (CD18) purified monoclonal (clone TS1/18) purchased from Endogen (Woburn, MA) and β7 integrins were R-phycoerythrin (R-PE)-conjugated rat anti-mouse integrin β7 chain monoclonal antibody (clone M293) purchased from PharmMingen (BD Biosciences, San Diego, CA). These were anti-human β2 integrin monoclonal and PE anti-mouse integrin β7. The anti-β7 blocking antibody can cross-react with human adhesion molecules (Kilshaw and Murant, 1991). Cells were incubated with these antibodies on ice for at least 30 min in a 12 $\times$ 75 mm Falcon tube (Becton-Dickinson, Franklin Lakes, NJ).

Site density of adhesion molecules

The expression of VLA-4 and VCAM-1 adhesion molecules was measured with fluorescent mAbs and quantified using a standard curve generated with Quantum Simply Cellular microsphere (Bangs Laboratories, Fishers, IN). These microspheres were stained with the same VLA-4 and VCAM-1 mAb and analyzed in parallel. The number of VLA-4 and VCAM-1 sites per cell was found to be constant over time at (56,000 $\pm$ 8200) and (586,000 $\pm$ 140,000), respectively.

Cell preparation

B78H1 cells were harvested when they were 90% confluent. On the day of the experiment, the cells were incubated for 5 min at 37°C in 5 ml of 0.526 mM solution of EDTA (Irvine Scientific, Santa Ana, CA). After incubation, 5 ml of RPMI media were added to the cell flasks and then the cell solution was pipetted to a 50-ml vial. Cells in this solution were separated from the medium by centrifuging the vials at 1400 RPM (394 $\times$ g) for 10 min at 4°C. Supernatant was removed and the cells were resuspended with RPMI. B78H1 cells were stained with CFSE (Molecular Probes, Eugene, OR: 5-(and-6)-carboxyfluorescein diacetate, succinimidyl ester (5(6)-CFDA, SE; CFSE: emission 517 nm) in 10-μM final concentration and incubated for 20 min at 37°C. Flow cytometric detection of U937 was done with hydroethidine (Molecular Probes: emission 620 nm) stained cells (2 μM final concentration) and incubated for 20 min at 37°C. Those cells were then separated from the solution by centrifuging the sample at 1400 RPM at 4°C, for 10 min. The sample was washed two more times, once with 3 ml of EDTA and once with 3 ml of HHB (110 mM NaCl, 10 mM KCI, 10 mM glucose, 1 mM, $MgCl_2$, and 30 mM HEPES, pH 7.4) and supplemented with 0.1% Human Serum Albumin (Bayer, Elkhart, IN), then resuspended with HHB. The cells were counted using a Z2-Coulter counter (Coulter, Miami, FL). At least 30 min before performing the experiment, the cells were incubated on ice with TS1/18 (anti-β2) to block CD18 adhesive contributions.

Before mixing the B78H1 and U937 cells together, the cells were incubated at 37°C for 5 min. U937 cells were incubated in HHB buffer having a cation content of 1 mM Mn^{2+}, 1 mM Mn^{2+} + 1 mM Ca^{2+}, 1 mM Mn^{2+} + 10 mM Ca^{2+}, 1 mM Ca^{2+}, or no ions. Then the two cell populations were combined with 3 $\times$ 10^6 B78H1 cells and 1.0 $\times$ 10^6 U937 cells per ml. A 0.5 $\times$ 2 mm magnetic stir bar was placed in a polystyrene tube and the bar was rotated at 300 RPM. The polystyrene tube was placed in a waterbath cup and maintained at 37°C. The waterbath holder and polystyrene tube were coupled to a flow cytometer. The sample was stirred for 4.0, 1.0, and 0.5 min and then the magnetic stir bar was turned off. Although variable, shear conditions within the test tube were sufficient to produce substantial cellular aggregates. We have performed disaggregation experiments using the stir bar at 300 RPM and found disaggregation rates similar to constant shear conditions of 800 s^{-1} (data not shown) in a parallel ring viscometer.

Then LDV-containing small molecule was added to the solution, the solution was mixed gently, and then the water-bath holder and polystyrene tube were coupled to the flow cytometer. Four 12-min continuous time-course measurements were taken for each ionic condition. For confocal microscopy (Zeiss 510 Laser Scanning Microscope, Thornwood, NY), stained cells were stirred 4.0 to 0.5 min and added to a deionized water

solution containing 2% paraformaldehyde and 10% phosphate buffer solution.

Molecular kinetic analysis

Molecular dissociation measurements of VLA-4 were made using the specific ligand, the FITC conjugated derivative of the LDV-containing small molecule (4-((*n*′-2-methylphenyl)ureido)-phenylacetyl-L-leucyl-L-aspartyl-L-valyl-L-prolyl-L-alanyl-L-alanyl-L-lysine) or rhVCAM-1-FITC as described previously (Chigaev et al., 2003a,b). Human monoblastoid U937 cells (1×10^6 cells/ml) expressing VLA-4 were preincubated in HEPES buffer for 10 to 30 min at 37°C with the same divalent cation conditions as in cell aggregation analysis. To measure ligand dissociation rates, the small fluorescent ligand or rhVCAM-1-FITC was preincubated with U937 cells and dissociation was initiated with excess unlabeled LDV-containing small molecule as described previously (Chigaev et al., 2003a,b). Competitive binding experiments were performed with the native ligand, soluble recombinant human vascular adhesion molecule 1 (rhVCAM-1), and the fluorescent small molecule and analyzed to obtain rate constants of the native molecule (Sklar et al., 1985; Chigaev et al., 2003).

Flow cytometry

Flow cytometric analysis was done on a Becton-Dickinson FACScan flow cytometer (Becton-Dickinson). Data acquisition was performed using CellQuest (Becton-Dickinson) and a Power Macintosh G4. Instrument settings (PMT voltages, amplifier gains, and compensation) were set to give the best separation between U937, B78H1, and aggregate populations as shown in Fig. 1. B78H1 cells (labeled with CFSE that emits at 517 nm) are detected by FL1. U937 cells (labeled with hydroethidine that emits at 605 nm) are detected by FL2. Aggregates formed from a combination of B78H1 and U937 are detected in both FL1 and FL2 detectors. In a plot of the FL1 and FL2 signals, three populations appeared: singlets populations involving B78H1 cells, singlet populations involving U937 cells, and an aggregate population that contained bound U937 and B78H1 cells.

Data were analyzed offline using Windows Multiple Document Interface Flow Cytometry Interface (Scripps, La Jolla, CA), which is a PC version of Cell Quest. Populations of U937, B78H1, and aggregate were selected. The count rates for each of the three populations were obtained. Ratio of counts between aggregates, U937, and B78H1 were obtained. Percentage of aggregate formation (*Agg%*) was determined for aggregates relative to U937 cells as

$$Agg\% = (Agg/[Agg + U937]) \times 100, \qquad (1)$$

where *Agg* and *U937* represent the number of aggregates and U937 cells obtained from FL1 and FL2 plots. Equation 1 was then plotted as a function of time and a least-square fit on these data was used to extract the disaggregation rate constant (k_{disagg}). The fits were done using GRAPHPAD PRISM (San Diego, CA) with one or two exponential decay terms.

Estimating number of cell aggregation adhesion bonds

Single bond dissociation rate for a bound ligand [*A*]* decaying to an unbound ligand [*A*] can be expressed as $[A]^* \xrightarrow{k_1} [A]$. The rate of depletion of bound ligand as a function of time (dissociation rate) is

$$d[A]^* = -[A]^* \times k_1 \times \mathrm{dt} \Rightarrow [A]^*_t = [A]^*_o \times e^{-k_1 t}, \qquad (2)$$

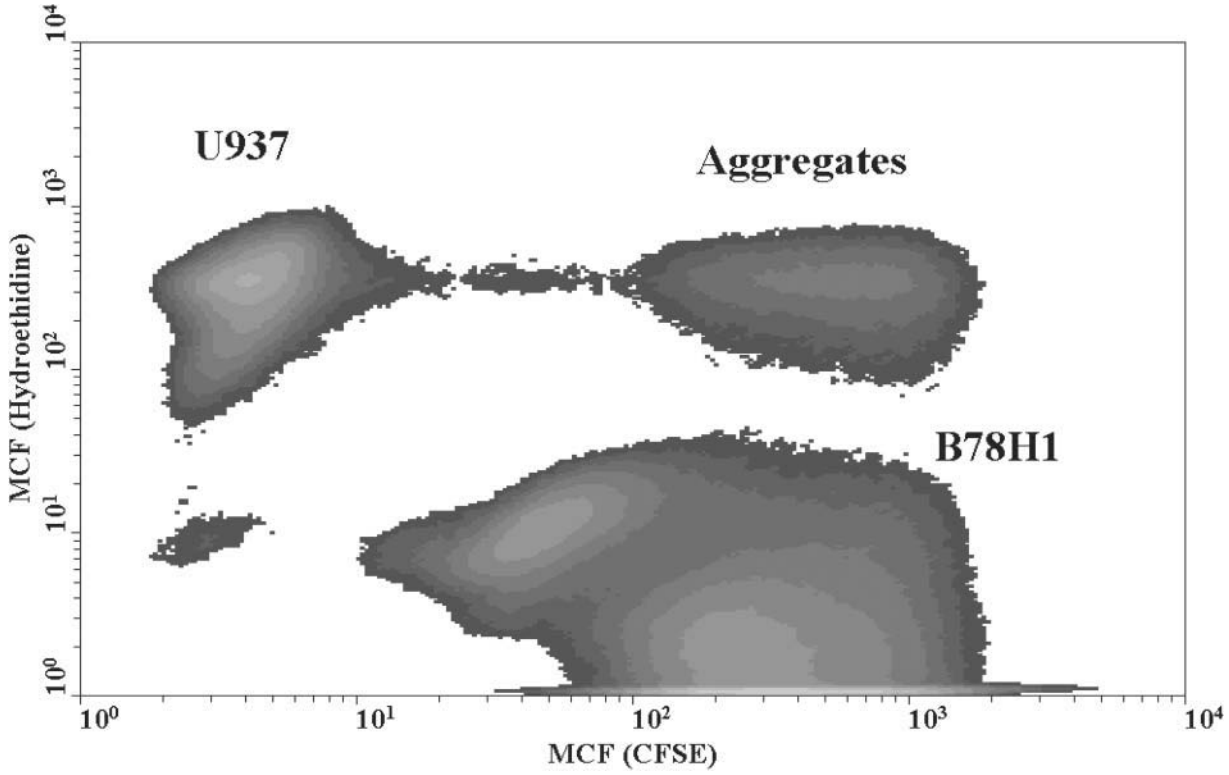

FIGURE 1 A white and black dot plot of flow cytometric analysis of aggregation. Each cell or aggregate is characterized in terms of green FL1 (*x* axis) and red FL2 (*y* axis) fluorescence. Singlet populations are B78H1 (stained with CFSE; green) and U937 (hydroethidine; red) cells and aggregates are a combination of these two types of colors. For illustration, white and black regions represent high and low count densities, respectively.

where $[A]^*_o$ is the initial concentration of bound ligands, $[A]^*_t$ is the number of bound ligand at time t, and k_1 is a dissociation constant. The probability of having free ligand after adding excess monovalent competitor is defined as

$$FFL = ([A]^*_o - [A]^*_t)/[A]^*_o = 1 - e^{-k_1 t}. \quad (3)$$

Equation 3 can be extended to n bonds binding a ligand to a receptor, provided that the dissociation rates for each bond are independent of one another and equal. This condition is true when no shear forces are acting on the bonds. Then the total probability of forming free ligands by multiplication of all dissociation probabilities for each bond is

$$FFL_n = (1 - e^{-k_1 t})^n. \quad (4)$$

The half-life for a ligand bound n times is defined as

$$t_{1/2}(n) = \ln[2]/k_n, \quad (5)$$

where k_n is the multiple bond dissociation rate. Then Eq. 4 can be written as

$$0.5 = (1 - e^{-k_1 t_{1/2}(n)})^n. \quad (6)$$

Equation 6 becomes

$$\ln[1.0 - 0.5^{1/n}] = -k_1 x\, t_{1/2}(n) = -k_1 x(\ln[2]/k_n). \quad (7)$$

A ratio of single dissociation rate (k_1) to that of multiple bond dissociation rates (k_n) is defined as X_f and yields

$$X_f = k_1/k_n = \ln[1.0 - 0.5^{1/n}]/\ln[0.5] = \log[1.0 - 0.5^{1/n}]/\log[0.5]. \quad (8)$$

Equation 8 can be used to relate the observed cellular disaggregation rate and molecular dissociation rate constants provided that shear forces acting on the bonds are negligible.

RESULTS

Measurement of cellular disaggregation

Several affinity states of VLA-4 were prepared by incubating U937 cells for 5 min at 37°C in solutions of HHB containing divalent cations, listed from high to low affinity: Mn^{2+} (1 mM concentration), Mn^{2+} and Ca^{2+} (1 mM concentration each), 1 mM Mn^{2+} and 10 mM Ca^{2+}, 1 mM Ca^{2+}, and no ions. The U937 and B78H1 cells were combined and stirred for 4 min at 37°C, then the stir bar was turned off and LDV-containing small molecule was added. Results from these adhesive experiments are shown in Fig. 2 *A*. Because different rates of disaggregation are observed, these findings suggest that cellular avidity is a function of the divalent cations. The relative differences in disaggregation rates mirror previous affinity measurements (Chigaev et al., 2003a).

The data in Fig. 2 *A* also show that disaggregation has a fast and slow component. This is most clearly shown for the 1 mM Mn^{2+} + 1 mM Ca^{2+} dissociation experiment. We evaluated the potential sources of the two components. To determine if there were additional adhesion molecules responsible for the second decay component, antibodies blocking $\beta 2$ and $\beta 7$ integrins (integrins known to potentially cooperate in cell aggregation) were added to U937 cells at

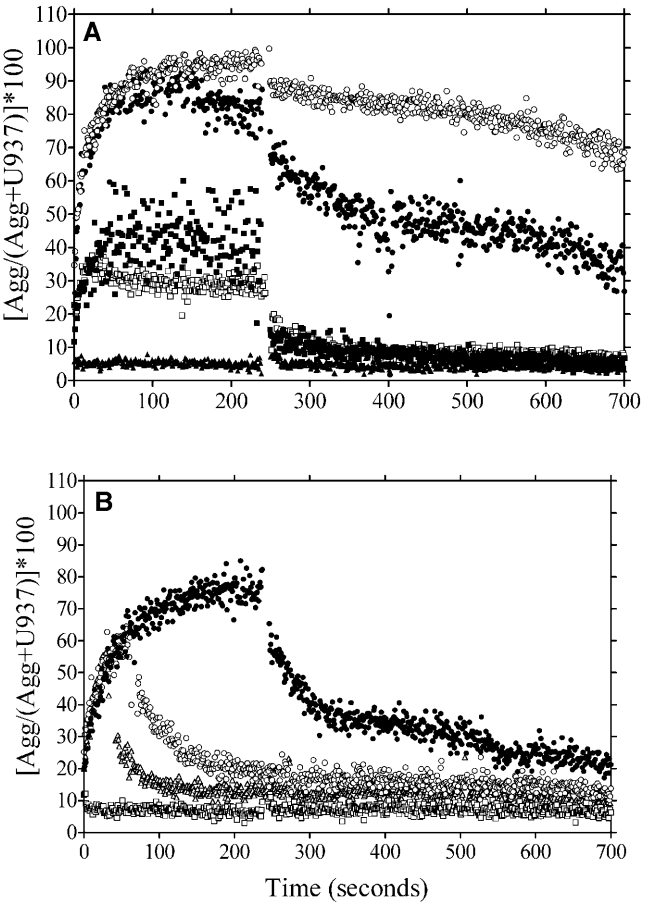

FIGURE 2 (*A*) Aggregate formation versus time for five affinity conditions of VLA-4 after 4.0 min of stirring. After 4 min, LDV-containing small molecule was added and the magnetic stir was turned off. The open circles represent 1 mM Mn^{2+}, the solid circles represent 1 mM Mn^{2+} and 1 mM Ca^{2+}, the solid squares represent 1 mM Mn^{2+} + 10 mM Ca^{2+}, the open squares represent 1 mM Ca^{2+}, and the solid triangles represent no-ions. (*B*) Aggregation formation and breakup for variable periods of aggregate formation in (1 mM Mn^{2+} and 1 mM Ca^{2+}). The sample used stirring times of 4.0 (*solid circles*), 1.0 (*open circles*), and 0.5 (*open triangles*) min. Also shown is a control sample in which aggregation was blocked by preaddition of LDV-containing small molecule (*open squares*). After each stirring condition the LDV-containing small molecule was added and the magnetic stir was turned off.

100 μg/ml. The cells were mixed in the presence of 1 mM Mn^{2+} + 1 mM Ca^{2+} for 5 min at 37°C. No effect of adding the blocking antibodies was observed (data not shown).

We had initially assumed that a cell concentration of 4×10^6 cells/ml and a ratio between B78H1 and U937 of 3:1 would result in aggregates composed mostly of doublets or slightly larger cell clusters containing one U937 cell. To examine the possibility that aggregate size varies over time and that the magnitude of the fast and slow disaggregation components were sensitive to aggregate size, we examined disaggregation for samples stirred for 4.0, 1.0, and 0.5 min (Fig. 2 *B*) while using microscopy in parallel (Fig. 3). Results are shown for the intermediate state formed in 1 mM Mn^{2+}

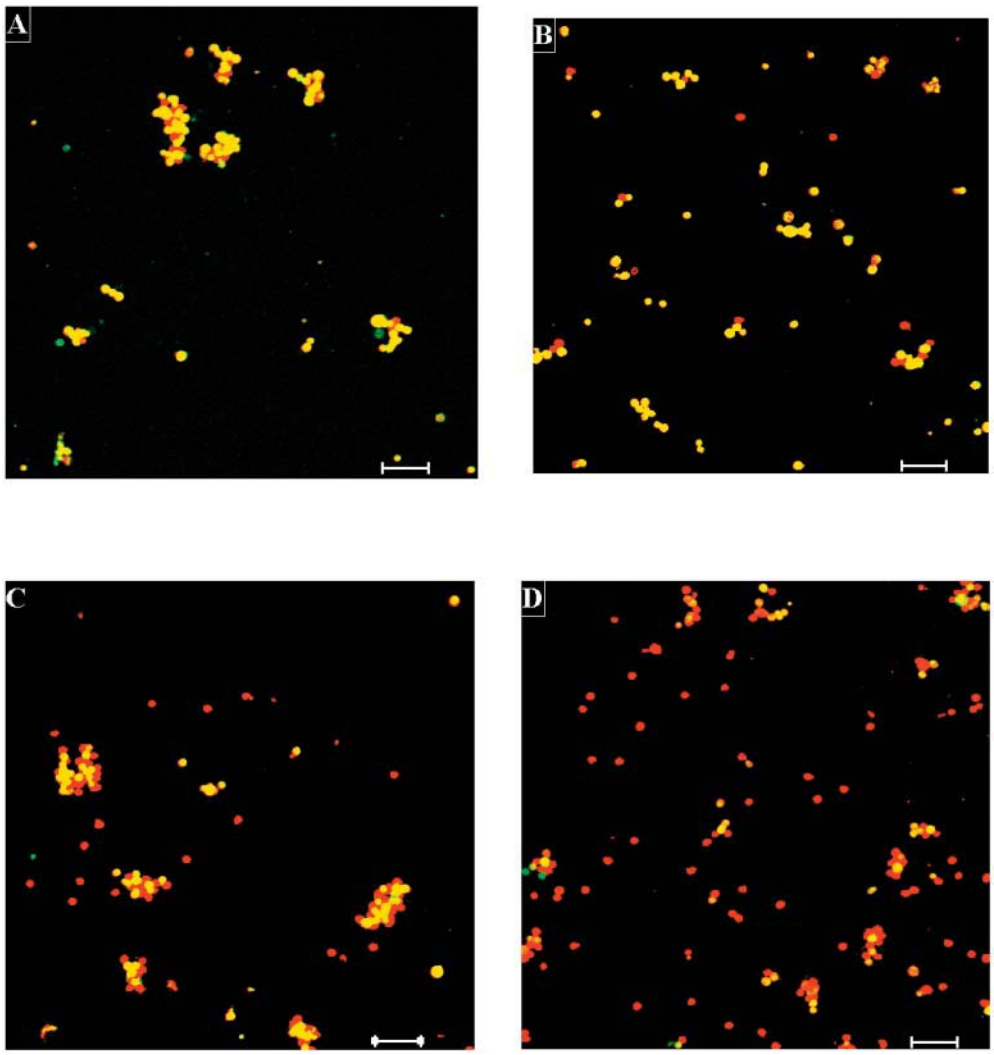

FIGURE 3 Aggregate formation observed by microscopy. Confocal images of B78H1 (*green/yellow images*), U937 (*red images*), and aggregates at 4.0 (*A*) and 0.5 (*B*) min stirring time formed at a 3:1 ratio between B78H1 and U937. U937 cells were incubated in the presence of 1 mM Mn^{2+} + 1 mM Ca^{2+} in HBB. *C* and *D* represent 4.0 and 0.5 stirring times for a ratio of 1:3 B78H1 to U937. A 100-μm unit length bar is added to the figures to show sizes of aggregates. Typical cell size is 15 μm. The experiment was repeated on three occasions with at least 40 photographs taken each time.

and 1 mM Ca^{2+}. Table 1 shows the disaggregation rate constants that were obtained from these measurements. Also see Table 1 for dissociation rates of experiments. The fast and slow components for each of the respective stirring times showed similar rates regardless of stirring duration, but the magnitude of the slow component increased over time.

Conditions for analysis of small aggregates

Although disaggregation rates remained similar with stirring duration, observation under the microscope showed that aggregate size varied considerably. Confocal microscopy was used to examine the aggregates to determine whether small (<4 cells) and large (>20 cells) clusters formed (see Fig. 3). The first set of images was taken of B78H1 and U937 cells combined in a 3:1 ratio and then stirred with a magnetic stir bar at 300 RPM for 4.0 and 0.5 min (Fig. 3, *A* and *B*). The large aggregates were formed preferentially over time. At 0.5 min, small clusters were composed of small numbers of B78H1 cells or a combination of B78H1 and U937 cells. At 4.0 min, there were two types of clusters. The large clusters consisted of many B78H1 cells with zero, one, or two U937 cells embedded in the cluster. The B78H1 cells aggregate homotypically and as a result, B78H1 clusters collect U937 cells and embed them inside. These images provide direct evidence for the presence of large aggregates in which U937 cells are embedded after longer stirring. When the U937 cells are embedded inside the large B78H1 clusters, it is probable that the VLA-4 and VCAM-1 adhesion bonds are protected from shear stresses and blocking peptides.

When the ratio of B78H1 cells to U937 cells was 1:3 (Fig. 3, *C* and *D*), at 0.5 min, a few large aggregates were observed and many small aggregates. Although U937 cells did not form homotypic aggregates, they did cluster around free B78H1 cells after 4.0 min of stirring. This type of cluster could protect the embedded B78H1 cell and its associated adhesion bonds. Taken together, the microscopy supports the concept of data resulting in large and small aggregates, with small aggregates dominating at early stirring times. We were unable to measure the aggregate size distribution using a Z2-

TABLE 1 Comparison of disaggregation rates after 4.0, 1.0, and 0.5 min of stirring in the presence of 1 mM Mn^{2+} + 1 mM Ca^{2+}, and then LDV-containing small molecule was added to block VLA-4 and VCAM-1 bonds

	4 min (fast)	4 min (slow)	1 min (fast)	1 min (slow)	0.5 min (fast)	0.5 min (slow)
k_{disagg} ($\times 10^{-4}$ 1/s)	331 ± 27	23 ± 1.0	279 ± 11	12 ± 1.0	520 ± 18	15.0 ± 0.6
$t_{1/2}$ (s)	20.9 ± 1.7	300 ± 13	24.8 ± 1.0	577 ± 48	13.3 ± 0.5	462 ± 18

Data is from two sets of experiments.

Coulter counter or the flow cytometer. The particle size resolution was not sufficiently adequate to resolve the wide range of aggregate sizes observed in the confocal images.

For subsequent measurements, we minimized the effect of large homotypic B78H1 aggregates by reducing the mixing time from 4 min to 0.5 min and using B78H1 and U937 cells combined in a 1:3 ratio. Fig. 3 *D* shows the absence of large aggregates when minimizing homotypic aggregation. Fig. 2 *B* shows that after the addition of LDV-containing small molecule (specific to VLA-4) the aggregates immediately broke up, suggesting that VLA-4/VCAM-1 bonds were the only bonds holding the aggregates together. Fig. 4 shows the disaggregation rates for three affinity states measured after 0.5 min stirring times under conditions dominated by small aggregates. After 0.5 min, the magnetic stir bar was turned off (simulating an environment without shear stress) and then LDV-containing small molecule was added. The data are plotted as the percentage of aggregates with respect to U937 singlets over time.

Table 2 compares the cellular disaggregation rates as observed in Fig. 4 for the three highest affinity states of VLA-4 to the monomeric ligand dissociation rates obtained under the same ionic conditions. Also shown in Table 2 are errors, associated values of goodness of fits, and half-life ($t_{1/2} = 0.693/k_{off}$). The k_{off} values were obtained either by direct measurements with VCAM-1-FITC or by competitive measurements with the native ligand and a fluorescent LDV-containing small molecule. The variation between the highest and lowest affinity states is a factor of ~20. The variation between the two methods of determination is a factor of ~2.

The cellular rates were determined for the three affinity states under three conditions. The conditions included live or fixed cell determination of disaggregation with B78H1 cells that express VCAM-1 only. In addition, experiments between CHO-VCAM-1 transfectants and U937 cells were analogous as long as the potential β2-integrin/ICAM interaction was inhibited by TS2/16 blocking antibody (see Table 2). We have also examined the appearance of U937 singlets from the live cell data and found their appearance rate to be the same as the disappearance of aggregates (data not shown). The results indicate that the cell disaggregation rates vary by a factor of 15 to 20 between the highest and lowest affinity forms, that the rates are comparable regardless of analysis condition, and that rates are similar to those reported for monomeric native ligand. Based on Eq. 8, the calculated number of VLA-4/VCAM-1 bonds is small for cell aggregates.

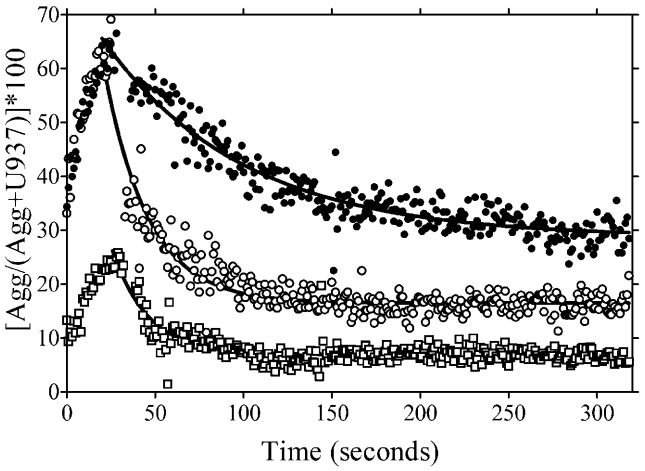

FIGURE 4 Percentage of aggregates with respect to U937 singlet cells over time for three affinity states. After 0.5 min of stirring, LDV-containing small molecule was added and the magnetic stir was turned off. Solid circles represent 1 mM Mn^{2+}, open circles represent 1 mM Mn^{2+} + 1 mM Ca^{2+}, and open squares represent 1 mM Mn^{2+} + 10 mM Ca^{2+}. Solid curves are best-fit to data and results are given in Table 2.

DISCUSSION

Cellular disaggregation

Measurements of k_{disagg} may depend on technique (parallel plate flow chamber, micropipette technique, or shear stress experiments where cells are in suspension) because both the force acting on the adhesion bonds and its rate of application control the dissociation rate once the bonds are formed. The simplest approach to obtain k_{off} rates for adhesion molecules from cellular aggregate experiments is to create single adhesion bond conditions. Other laboratories have tried to create single bond environments by reducing the number of receptors and ligands to a level where single or few adhesion bonds are formed. Then this low bond system was studied under a defined force. It is not clear, however, if single bond conditions were formed, or their physiological significance. For example, micropipette techniques can accurately control time of contact, force acting on bonds, number of receptors and ligands available for binding, and cell-cell contact area. However, the length of time that the cells are in contact, the mechanical means in which cells separate, and the low receptor site density do not necessarily represent the

TABLE 2 Comparison of cellular disaggregation rates to dissociation rates obtained from experiments using rhVCAM-1 and U937 cells after 0.5 min of stirring at three affinity states of VLA-4

Condition		Mn^{2+}	Mn^{2+} + Ca^{2+}	Mn^{2+} + 10 mM Ca^{2+}
Monomeric ligand	k_{off} – rhVCAM-1 ($\times 10^{-4}$ 1/s)*	140 ± 20	360 ± 20	—
	$t_{1/2}$ – rhVCAM-1 (s)*	50 ± 7	19 ± 1	—
	k_{off} – rhVCAM-FITC ($\times 10^{-4}$ 1/s)†	340 ± 50	650 ± 11	(12200 ± 320)‡
	$t_{1/2}$ – rhVCAM-FITC (s)†	20 ± 3	11 ± 2	(0.57 ± 0.02)‡
Live B78H1-U937	k_{disagg} – aggregates ($\times 10^{-4}$ 1/s)	183 ± 19	393 ± 22	>2497
($N = 3$)	$t_{1/2}$ – aggregates (s)	38 ± 4	18 ± 1	<2.8
Fixed B78H1-U937	k_{disagg} – aggregates ($\times 10^{-4}$ 1/s)	159 ± 42	514 ± 186	>2088
($N = 3$)	$t_{1/2}$ – aggregates (s)	44 ± 12	13 ± 5	<3.3
Live CHO-U937	k_{disagg} – aggregates ($\times 10^{-4}$ 1/s)	153 ± 65	378 ± 43	>2970
($N = 3$)	$t_{1/2}$ – aggregates (s)	45 ± 2	18 ± 2	<2.3
Cellular average	k_{disagg} – aggregates ($\times 10^{-4}$ 1/s)	165 ± 43	428 ± 9	>2518
	$t_{1/2}$ – aggregates (s)	42 ± 11	16 ± 4	<2.3 (live)
Ratio of single dissociation rate to that of multiple bond dissociation rate	X_f (aggregate-rhVCAM-1)	0.8 ± 0.2	0.8 + 0.1	—
	X_f (aggregate-rhVCAM-FITC)	2.5 ± 0.6	1.6 + 0.1	<4.1
Number of bonds	(Using rhVCAM-1)	0.9 ± 0.2	0.8 ± 0.1	—
	(Using rhVCAM-FITC)	2.6 ± 1.8	1.8 ± 0.1	<11.6

Data obtained from percentage of aggregation with respect to U937 cells and percentage of U937 cells with respect to number of aggregates. The errors reflect the standard error in mean of curves fitted to the data. Number of experimental measurements obtained is denoted by *N*.

*Data from competitive binding experiments using LDV-FITC-containing small molecule as a ligand and nonlabeled rhVCAM-1 as a competitor. Those results represent the natural ligand dissociation rates for monomeric VCAM-1.

†Data obtained from rhVCAM-FITC dissociation experiments.

‡Data obtained using rapid mix flow cytometry (Graves et al., 2002). Monomeric ligand results are data from Chigaev et al. (2003a). Bond number and X_f are upper limits due to the minimum time required to handle samples.

timescale, forces, or receptor densities that adhesion bonds would experience while in a capillary vessel.

We have chosen an alternative method to obtain cellular disaggregation constants that can be compared to molecular rates when cellular aggregates are in a no-fluid-shear force environment. This condition simulates the same environment that molecular peptides experience for experiments that measure molecular adhesion k_{off} rates. To prevent molecular rebinding during the cellular disaggregation phase a blocking peptide was used. A possible limitation of performing an experiment without shear forces is that a shear stress is generated when the flow cytometer siphoned samples from a polystyrene tube at 0.6 μl/s through 180 μm (0.007'') inner diameter tubing. The shear rate at the walls of the tubing is given by Whorlow (1992) as

$$S_{wall} = 4 \times Q/\pi \times r^3. \quad (9)$$

Q is the flow rate (μl/s) and r is the radius of the tube through which the cells are flowing. Equation 9 estimates shear rate of 442 s^{-1} at the wall.

We repeated the experiments to minimize the effect of shear forces that arise during the 5-s transit time through the FACScan. Pipette tips were cut off to a diameter ~0.5 cm (where wall shear is negligible—10 s^{-1}) and used to remove manually 50 μl of aggregated cell samples at 5- or 10-s intervals after peptide addition. Those samples were placed in 200 μl of 2% PFA and singlet and aggregate populations were examined with a FACScan. Table 2 gives the disaggregation rates using this method for three affinity conditions. The measured k_{disagg} rates are similar to the rates observed on live cells transported to the flow cytometer and both are similar to the monomeric ligand dissociation rates. This suggests that shear forces generated in transit do not impact the observed results. To illustrate that the disaggregation rates measured with B78H1 and U937 cells were due to VLA-4/VCAM-1 molecules we have also examined the k_{disagg} for CHO-VCAM-1 and U937 cells. U937 singlet appearance rate and the disaggregation rate were measured and the average of those measurements for the three affinity states are shown in Table 2. These rates were found to be similar to those found for the B78H1-VLA-4 and monomeric ligand experiments. Results for the 1 mM Mn^{2+} + 10 mM Ca^{2+} condition was an upper limit due to minimum time required to handle samples. This indicates that the disaggregation rates are VCAM-1/VLA-4 related and not due to other adhesion bond types.

Fig. 2 *A* shows that for the two highest affinity states of VLA-4 (1 mM Mn^{2+}, 1 mM Mn^{2+} +1 mM Ca^{2+}) there are fast and slow disaggregation rates. In the presence of the lowest affinity state (1 mM Mn^{2+} + 10 mM Ca^{2+}) there is a single component. Three possible explanations for the two-component behavior—another adhesion receptor-ligand pair, site density, and aggregate size—were explored. Because human monoblastoid U937 cells are known to express integrins other than VLA-4 (Prieto et al., 1994), such as $\alpha 4\beta 7$ (in low quantities) and Mac-1 and LFA-1 β_2-integrins, we verified that blocking mAbs did not alter

the disaggregation characteristics. Two cell populations, one expressing higher and one expressing lower levels of adhesion molecules might contribute the presence of two rates. No such distinct populations were observed by flow cytometric analysis of antibody binding to VLA-4 or VCAM-1 (data not shown).

We also examined the possibility that the size of cell aggregates could induce the presence of fast and slow disaggregation rates. We first determined whether the time allowed for aggregation regulated the fast and slow components. These experiments were performed on a state of VLA-4 (1 mM Mn^{2+} + 1 mM Ca^{2+}) where the two components are easily observed. According to Smoluchowski (1917) the number of cell-cell collisions is dependent on the length of time cells are stirred and the frequency is dependent on cell concentration, shear rate, and size of the cells. Given longer stirring times, larger aggregates could form. Fig. 2 *B* shows that the amplitude of the slow component increases with the duration of shear, and as shown under the microscope (Fig. 3), qualitatively corresponds to increased aggregate size. We thus attribute the slow rate to the large aggregates and the fast rates to smaller aggregates. The experiments were optimized for the formation of small aggregates, as is illustrated in Fig. 3. Fig. 2 shows the effect of reducing the stirring time on the elimination of larger aggregates on the dissociation curves. Performing experiments with 30-s mixing time minimizes the presence of large aggregates so when LDV-containing small molecule is added, the problem of large aggregates sheltering bonds is reduced. Using a blocking peptide, a small molecule, is the definitive approach for optimizing access to the binding sites. Thus, the cellular dissociation rate observed under these conditions is an upper limit to the actual dissociation rate.

Affinity and avidity

To study the relationship between VLA-4 affinity for VCAM-1 and cellular adhesive avidity, we selected the shortest period of aggregate formation (0.5 min) that would allow formation for the three highest affinity receptors. The disaggregation data were analyzed for aggregate breakup and compared to VCAM-1 dissociation rates. The similarity observed for the kinetics of disaggregation and data taken with soluble rhVCAM-1 lends credence to the idea that the short half-time relates to bond breakage in individual cells. Table 2 shows that the cellular disaggregation was, on average, 1.3 ± 0.4 times slower than the dissociation of monomeric ligands for the 1 mM Mn^{2+} and 1 mM Mn^{2+} + 1 mM Ca^{2+} conditions. Since cell-cell aggregates can form more adhesive bonds than the single one formed between VLA-4 and monomeric VCAM–1, slower cellular disaggregation is expected.

Integrin dissociation rates are typically at least an order-of-magnitude less than selectin rates (Bhatia et al., 2003). VLA-4 dissociation rates (0.02–0.2/s) are comparable to other integrin dissociation rates ($\alpha4\beta7$-MADCAM, 0.05–1.3/s; Château et al., 2001). High dissociation rates for adhesion molecules are usually associated with cell rolling whereas small dissociation rates are associated with firm cellular adhesion. Unlike selectins, integrins can have bond dissociation rates that are affinity-dependent. We found that for low VLA-4 affinity states, the dissociation rates tend toward selectin rates (P-selectin-PSGL-1, 2.4/s; Smith et al., 1999). High affinity state have bond dissociation rates that tend toward integrin values. This feature allows VLA-4 to be potentially active in both cell rolling and in firm adhesion, depending on the conformational state of the molecule.

Equation 8 relates the multivalent dissociation rate constant to the number of bonds involved in holding objects together as X_f, which is the ratio of single dissociation rate to that of multiple bond dissociation rate. This factor explicitly relates the observed cellular disaggregation rate and molecular dissociation rate constants. It is worth noting that this treatment applies under conditions where the addition of excess LDV-containing small molecule prevents rebinding between VLA-4 and VCAM-1 once the bond is broken. Fig. 5 shows the values generated using Eq. 8. From Table 2 an average X_f value was found to be 1.3 ± 0.4 for the 1 mM Mn^{2+} and 1 mM Mn^{2+} + 1 mM Ca^{2+} conditions. Entering this value into Eq. 8 yields a predicted number of bonds of 1.5 ± 0.7. As the bulk disaggregation rate including large aggregates must be viewed as an upper limit to the disaggregation of doublets into singlets, the bond estimate is also an upper limit. This low bond number estimate is consistent with low bond number predictions from other adhesion experiments that used CD16a (Chesla et al., 1998), E-selectin (Piper et al., 1998), swollen red cells expressing blood group B antigen cross-linked by monoclonal anti-B antigen IgM antibody (Long et al., 1999), fibroblasts bound to fibronectin (Thoumine et al., 2000), and E-selectin constructs (Long et al., 2001). Our data also suggests that

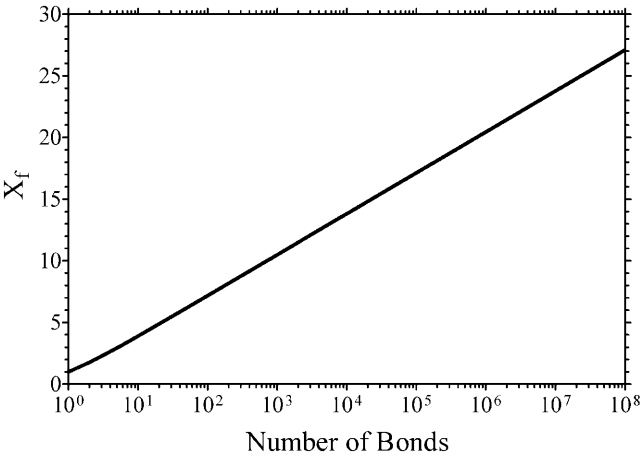

FIGURE 5 Predicted rate dissociation constant ratio X_f that compares single dissociation rate to that of multiple bond dissociation rate as a function of bond number.

the low number of bonds holding an aggregate together is not strongly dependent on the affinity of VLA-4, although the rapid dissociation of the lowest affinity state leads to the greatest measurement uncertainty. The nominal bond number of ~12 for the 1 mM Mn^{2+} + 10 mM Ca^{2+} condition is an upper limit due to the minimum time for sample handling (5 s) in cell disaggregation experiments. We conclude that 1–12 bonds may be holding cellular aggregates together in the lowest affinity state. It is possible that the low affinity state may require more bonds to form a stable aggregate compared to a few stronger bonds of a high affinity state. Regardless, low bond number appears to exclude the possibility that more adhesion bonds are responsible for an increase in number of aggregates as the affinity state of VLA-4 is increased (Fig. 2 *A* and Fig. 4).

Bond clustering

Recent experiments (Chigaev et al., 2003b; Takagi et al., 2002) have shown that with the addition of divalent cations VLA-4 extends from a folded resting state, where the binding site is near the cell surface, to an activated, upright state, in which the binding site of VLA-4 is readily exposed to other ligands. Since our results suggest that the binding of aggregates is the result of at most a few bonds, the potential impact of clustering of adhesion molecules activated by Mn^{2+} or Ca^{2+} could be minimal. We considered the possibility that the long disaggregation rates observed after 4 min of stirring could be attributed to the formation of a significant number of bonds, to bond clustering, or to sheltering of the bonds due to the size of the cell aggregate. Long stirring time could allow receptors and the complexes to cluster. Confocal images of U937 cells that were stimulated with Mn^{2+} did not detect bond clustering on the timescale of the stirring conditions for the experiments. For more bonds or receptor clusters to be responsible for the short and long disaggregation rates observed in Fig. 2 *B*, we examined the ratio between cell disaggregation rates and molecular dissociation rates and found a value of 42. Entering this value into Eq. 8, the predicted number of bonds is far larger than the number of adhesion molecules on the cells. The formation of large homotypic aggregates can shelter VCAM-1/VLA-4 bonds and provide for a slow disaggregation. This possibility was reduced by decreasing the stirring time to prevent the formation of large aggregates, as shown in Fig. 3. Thus the long disaggregation times are attributed to the size of the aggregate and its sheltering effect on bonds formed within the aggregate.

CONCLUSION

In the disaggregation of B78H1 and U937 aggregates, firm adhesion for cells in suspension could be mediated by changing the affinity state of VLA-4. This change in affinity leads to different values of the dissociation rate for VLA-4/VCAM-1 adhesive bonds. We estimate the number of adhesion bonds formed between cells by comparing values of the disaggregation rates of cells to dissociation rates of rhVCAM-1 and rhVCAM-FITC. The upper limit for the number of bonds holding cell aggregates together for the 1 mM Mn^{2+} and 1 mM Mn^{2+} + 1 mM Ca^{2+} conditions is (1.5 ± 0.7). Our estimation of the small number of bonds is consistent with previous experiments performed by other groups. Consequently cellular aggregates may require no more than a few bonds (two) to form and implies that cellular adhesion is driven by integrin affinity changes. Microscopy data show that the size of cell aggregates can affect the observed disaggregation rate.

This work was supported by National Institutes of Health (NIH) grants RR14175, 1EB002022, and HL56384 (to L.A.S.), and in part by a grant from the American Heart Association, 990318Z (to R.L.). Microscopy and flow cytometry were supported by NIH grant R2YCA88339 and the University of New Mexico Cancer Center.

REFERENCES

Alon, R., S. Chen, K. D. Puri, E. B. Finger, and T. A. Springer. 1997. The kinetics of L-selectin tethers and the mechanics of selectin-mediated rolling. *J. Cell Biol.* 138:1169–1180.

Bhatia, S. K., M. R. King, and D. A. Hammer. 2003. The state diagram for cell adhesion mediated by two receptors. *Biophys. J.* 84:2671–2690.

Brakebusch, C., D. Bouvard, F. Stanchi, T. Sakai, and R. Fassler. 2002. Integrins in invasive growth. *J. Clin. Invest.* 109:999–1006.

Chang, K. C., D. F. Tees, and D. A. Hammer. 2000. The state diagram for cell adhesion under flow: leukocyte rolling and firm adhesion. *Proc. Natl. Acad. Sci. USA.* 97:11262–11267.

Chateau, M., S. Chen, A. Salas, and T. A. Springer. 2001. Kinetic and mechanical basis of rolling through an integrin and novel Ca^{2+}-dependent rolling and Mg^{2+}-dependent firm adhesion modalities for the $\alpha4\beta7$-MAdCAM-1 interaction. *Biochemistry.* 40:13972–13979.

Chen, C., J. L. Mobley, O. Dwir, F. Shimron, V. Grabovsky, R. R. Lobb, Y. Shimizu, and R. Alon. 1999. High affinity very late antigen-4 subsets expressed on T cells are mandatory for spontaneous adhesion strengthening but not for rolling on VCAM-1 in shear flow. *J. Immunol.* 162:1084–1095.

Chesla, S. E., P. Selvaraj, and C. Zhu. 1998. Measuring two-dimensional receptor-ligand binding kinetics by micropipette. *Biophys. J.* 75:1553–1572.

Chigaev, A., A. M. Blenc, J. V. Braaten, N. Kumaraswamy, C. L. Kepley, R. P. Andrews, J. M. Oliver, B. S. Edwards, E. R. Prossnitz, R. S. Larson, and L. A. Sklar. 2001. Real-time analysis of the affinity regulation of $\alpha4$-integrin. The physiologically activated receptor is intermediate in affinity between resting and Mn^{2+} or antibody activation. *J. Biol. Chem.* 276:48670–48678.

Chigaev, A., G. J. Zwartz, S. W. Graves, D. C. Dwyer, H. Tsuji, T. D. Foutz, B. S. Edwards, E. R. Prossnitz, R. S. Larson, and L. A. Sklar. 2003a. $\alpha4\beta1$-Integrin affinity changes govern cell adhesion. *J. Biol. Chem.* M210472200. 278:38174–38182.

Chigaev, A., T. Buranda, D. C. Dwyer, E. R. Prozznitz, and L. A. Sklar. 2003b. FRET detection of cellular $\alpha4$ integrin conformational activation. *Biophys. J.* 85:3951–3962.

Chothia, C., and E. Y. Jones. 1997. The molecular structure of cell adhesion molecules. *Annu. Rev. Biochem.* 66:823–862.

Graves, S. W., J. P. Nolan, J. H. Jett, J. C. Martin, and L. A. Sklar. 2002. Nozzle design parameters and their effects on rapid sample delivery in flow cytometry. *Cytometry*. 47:127–137.

Haas, T. A., and E. F. Plow. 1994. Integrin-ligand interactions: a year in review. *Curr. Opin. Cell Biol.* 6:656–662.

Kilshaw, P. J., and S. J. Murant. 1991. Expression and regulation of $\beta 7(\beta p)$ integrins on mouse lymphocytes: relevance to the mucosal immune system. *Eur. J. Immunol.* 21:2591–2597.

Long, M., H. L. Goldsmith, D. F. Tees, and C. Zhu. 1999. Probabilistic modeling of shear-induced formation and breakage of doublets cross-linked by receptor-ligand bonds. *Biophys. J.* 76:1112–1128.

Long, M., H. Zhao, K. S. Huang, and C. Zhu. 2001. Kinetic measurements of cell surface E-selectin/carbohydrate ligand interactions. *Ann. Biomed. Eng.* 29:935–946.

McEver, R. P. 2001. Adhesive interactions of leukocytes, platelets, and the vessel wall during hemostasis and inflammation. *Thromb. Haemost.* 86:746–756.

Osborn, L., C. Hession, R. Tizard, C. Vassallo, S. Luhowskyj, G. Chi-Rosso, and R. Lobb. 1989. Direct expression cloning of vascular cell adhesion molecule 1, a cytokine-induced endothelial protein that binds to lymphocytes. *Cell.* 59:1203–1211.

Piper, J. W., R. A. Swerlick, and C. Zhu. 1998. Determining force dependence of two-dimensional receptor-ligand binding affinity by centrifugation. *Biophys. J.* 74:492–513.

Prieto, J., A. Eklund, and M. Patarroyo. 1994. Regulated expression of integrins and other adhesion molecules during differentiation of monocytes into macrophages. *Cell. Immunol.* 156:191–211.

Shyy, J. Y., and S. Chien. 2002. Role of integrins in endothelial mechanosensing of shear stress. *Circ. Res.* 91:769–775.

Sklar, L. A., J. Sayre, V. M. McNeil, and D. A Finney. 1985. Competitive binding kinetics in ligand-receptor-competitor systems. Rate parameters for unlabelled ligands for the formyl peptide receptor. *Mol. Pharmacol.* 28:323–333.

Smith, M. J., E. L. Berg, and M. B. Lawrence. 1999. A direct comparison of selectin-mediated transient, adhesive events using high temporal resolution. *Biophys. J.* 77:3371–3383.

Smoluchowski, M. V. 1917. Versuch einer mathematischen theorie der koagulationskienetik kolloider losungen. *Zeitschrift Phys. Chem.* 92: 129–168.

Takagi, J., B. Petre, T. Walz, and T. Springer. 2002. Global conformational rearrangements in integrin extracellular domains in outside-in and inside-out signaling. *Cell.* 110:599–611.

Thoumine, O., P. Kocian, A. Kottelat, and J. J. Meister. 2000. Short-term binding of fibroblasts to fibronectin: optical tweezers experiments and probabilistic analysis. *Eur. Biophys. J.* 29:398–408.

Whorlow, R. W. 1992. Tube viscometers. *In* Rheological Techniques. Ellis Horwood Limited, London, England. 43–96.

Zhu, C., M. Long, S. E. Chesla, and P. Bongrand. 2002. Measuring receptor/ligand interaction at the single-bond level: experimental and interpretative issues. *Ann. Biomed. Eng.* 30:305–314.